

## Research

### An evaluation of antimicrobial potency of silver nanoparticles synthesised from *Fusarium sp.*

Ngunjiri Vincent Mwangi<sup>1</sup> · Shigwenya Edwin Madivoli<sup>1</sup> · Mourine Kangogo<sup>2</sup> · Mwangi Clement Wangui<sup>1,3</sup> · Indire Sammy Wanakai<sup>1</sup> · Mwanza Dennis Nzilu<sup>1</sup> · Walyambillah Waudu<sup>1</sup>

Received: 5 December 2023 / Accepted: 27 March 2024

Published online: 06 April 2024

© The Author(s) 2024 [OPEN](#)

#### Abstract

Biological synthesis of metal nanoparticles has caught the interest of scientists due to the environment friendly synthesis approach which yields metallic nanoparticles with antimicrobial potency. In the present study silver nanoparticles were produced using a green method with the assistance of *Fusarium sp.* fungal cell filtrate and their antimicrobial potency was explored. The silver nanoparticles depicted a surface plasma resonance of 434 nm when run in the Ultra Violet–Visible Spectrophotometer. The functional group present in the nanoparticles were investigated using an Attenuated Total Reflectance-Fourier Transform Infrared where –OH, C–H, amide I and amide II functional groups were notable. The morphology and crystallinity of the produced silver nanoparticles was investigated with the help of a Scanning Electron Microscope and X-ray Diffraction. The X-ray diffraction results revealed that the nanoparticles were crystalline in nature with a face centred cubic structure and a crystallite size of 38.5 nm. The Scanning Electron Microscope revealed that the nanoparticles were spherical with sizes ranging between 3 to 43 nm. Antimicrobial studies of the synthesised silver nanoparticles were conducted at different concentrations (1 mM, 10 mM, 20 mM and 100 mM) against disease causing microorganisms *Bacillus subtilis*, *Staphylococcus aureus*, *Escherichia coli* and *Pseudomonas aeruginosa*, the results showed that at a concentration of 1 mM there was no inhibition but as the concentration was increased to 20 mM and 100 mM, there was a notable inhibition with the maximum inhibition zone being  $17 \pm 0.6$  mm.

#### Article highlights

- The study involved synthesis, optimization and characterization of silver nanoparticles that were produced with the help of *Fusarium sp.*
- Characterization of the silver nanoparticles revealed that the nanoparticles were crystalline and spherical in nature.
- The antimicrobial results indicated that the nanoparticles had notable inhibition zones meaning they can be applied as antimicrobials.

**Keywords** Silver nanoparticles · Synthesis · Cell filtrate

---

✉ Ngunjiri Vincent Mwangi, [ngunjirimmust@gmail.com](mailto:ngunjirimmust@gmail.com) | <sup>1</sup>Chemistry Department, Jomo Kenyatta University of Agriculture and Technology, P.O. Box 62000-00200, Nairobi, Kenya. <sup>2</sup>Medical Microbiology Department, Jomo Kenyatta University of Agriculture and Technology, P.O. Box 62000-00200, Nairobi, Kenya. <sup>3</sup>Department of Pharmaceutical Chemistry, Mount Kenya University, P.O. Box 342-01000, Thika, Kenya.



## 1 Introduction

Antimicrobial resistance has stood out to be among the major and urgent risks to human health which makes prevention and successful treatment of various ailments very difficult [1, 2]. Problems arising from antimicrobial resistance affect both the developing and developed nations posing great risks to public health [3]. Worldwide, the centre for disease control estimated that 4.95 million people lost their lives due to antimicrobial resistance related infections in 2019 [4]. To curb this menace, metal nanoparticles such as copper, zinc and silver are increasingly being utilized as antimicrobial agents as they have been shown to possess good inhibitory activity [5–7]. For instance, Herault et al. developed silver-containing titanium dioxide nanocapsules for combating multidrug-resistant bacteria. In their study, they observed that silver-containing titanium dioxide nanocapsules had strong antimicrobial activity against *Escherichia coli* and even against a multidrug-resistant strain of *Staphylococcus aureus* [8]. They demonstrated that the presence of the nanocapsules in macrophages that did not affect cell viability and did not activate proinflammatory responses at doses of up to 20 µg/mL [8]. With an aim to develop antimicrobial wound dressings, Madivoli et al., fabricated a stimuli responsive cellulose chitosan wound dressing containing zinc oxide nanoparticles. In the study, the authors observed that presence of zinc oxide entrapped within the polymeric network resulted in to inhibitory activity against *Escherichia coli* [9, 10]. On the mechanisms of action it has been postulated that nanoparticles do possess the potentiality to attach themselves on the plasma membrane via interactivity with the Coulomb force there by disrupting the plasma membrane [11, 12]. The triggering of a reactive oxygen species comprise of a mechanism where the nanoparticles induce disintegrations of microbial cells that only stop when the life of the microorganism is terminated [13–15].

In a study carried out by Ibrahim et al., it was observed that titanium oxide functionalized polystyrene nanocomposites exhibited good antimicrobial activities against *Staphylococcus aureus*, *Pseudomonas aeruginosa* [16]. Bayger et al. observed that medical sutures coated with biosynthesized silver nanoparticles were able to inhibit the growth of *Candida albicans*, *Escherichia coli* and *Staphylococcus aureus* [17]. Srisod et al. employed antimicrobial silver nanoparticles as a coatings which exhibited powerful and long lasting antibacterial properties against *Staphylococcus aureus* and *Escherichia coli* [18]. Jayakumar et al., developed polyvinyl alcohol antimicrobial fabrications by incorporating ZnO nanoparticles that had strong deterrence against *Staphylococcus aureus*, *Klebsiella pneumoniae* and *Pseudomonas aeruginosa* [19].

In another study Valenzuela et al., were able to obtain stable antimicrobial surfaces that were based on ZnO nanoparticles that had good proficiency against *Staphylococcus aureus* [20]. Turakhia et al., were able to fabricate cotton with copper oxide nanoparticles which was found to have promising antibacterial actions against *Escherichia coli* [21]. Another study by Acikbas and Calis Acikbas reported a modification of surfaces with copper oxide nanoparticles which showed good deterrence of *Staphylococcus aureus* and *Escherichia coli* [22]. In view of the potential antimicrobial activities portrayed by nanoparticles, this study therefore aimed at exploring and investigating the antimicrobial properties of silver nanoparticles synthesized using *Fusarium sp.* cell filtrate. The nanoparticles were characterized using an Ultra Violet Visible Spectrophotometer, an Attenuated Total Reflectance Fourier Transform Infrared, a Scanning Electron Microscope and by X-ray diffraction while their inhibitory activity against *Bacillus subtilis*, *Staphylococcus aureus* and *Pseudomonas aeruginosa* was evaluated using disc diffusion assay.

## 2 Materials and methods

### 2.1 Isolation of fungus

A soil sample was collected from Jomo Kenyatta University of Agriculture and Technology (JKUAT) farm in Juja, Kiambu County. The sample collection was done at a depth of 3–4 cm with the help of a spatula before taking the samples to JKUAT botany laboratory. 1 g of the soil sample was placed in 9 mL of sterile distilled water and was well shaken. Potato dextrose agar media was prepared by dissolving 39 g of the potato dextrose agar powder in 1000 mL distilled water which was supplemented with streptomycin, an antibiotic. The media was then sterilised by autoclaving at 15 lbs pressure and at 121 °C for fifteen minutes. Some fresh media was then poured into a petri dish where it solidified. 100 µl of the sample soil solution were placed on the potato dextrose agar plate, spread using a sterile

glass spreader, and then incubated at 28 °C for four days. After the 4 days of incubation sub-culturing was done using new potato dextrose agar plates. The plates were then incubated for 10 days at a temperature of 28 °C to allow development and growth of the fungal strain [23].

## 2.2 Characterization of the fungal strain

After the incubation period the fungal strain was identified based on its morphological characteristics. The characterization bench was cleaned using 70% alcohol whereas the lenses of the compound microscope were also cleaned using xylene. A sterile mounting needle was used to place the isolate on the slide and a drop of lacto-phenol dye was introduced before covering the slide with the cover slip. The slide was placed on the microscope and observation of the mycelia and the spore patterns was used for identification and characterization at a magnification of X40 under a compound microscope [24].

## 2.3 Fungal biomass production

To prepare potato dextrose broth media 24 g of the potato dextrose broth was dissolved in 1000 mL distilled water. The media was then divided in 250 mL portions and sterilised by autoclaving at 15 lbs pressure and at 121 °C for 15 min, *Fusarium sp.* was inoculated aseptically in the broth media using sterile mounting needles and were incubated at room temperature for 14 days. The produced biomass was then harvested by filtration through a sterilised muslin cloth and then washed with distilled water to ensure removal of any components of the growth media. The biomass wet weight measured was dissolved in 200 mL sterile distilled water. The flasks were then incubated at room temperature on a rotary shaker with 120 rotations per minute for 24 h. The biomass was filtered and the crude cell filtrate was collected for the use in the synthesis procedures [25].

## 2.4 Synthesis optimisation

To evaluate the effect of different reaction parameter on the synthesis of silver nanoparticles, the reaction time, concentration of silver nitrate solution, ratio of silver nitrate solution and the *Fusarium* cell filtrate, and the reaction temperature were evaluated. First, the effect of fungal filtrate amount on the synthesis of silver nanoparticles was studied by reacting 2 mM silver nitrate solution with different ratios of the *Fusarium* fungal cell filtrate (1:1–1:3) at 80 °C for an hour [26].

In order to determine the optimum concentration of the silver nitrate solution in the synthesis of the nanoparticles using *Fusarium sp.* 1 mM, 1.5 mM and 2 mM concentrations were prepared and were then reacted with the *Fusarium* fungal cell filtrate at a ratio of one is to one. The reaction time was maintained at one hour at a temperature of 80 °C. At the close of each reaction, the absorbance was measured and the spectrum obtained was recorded [27].

The optimum temperature was investigated by subjecting the silver nitrate solution and the *Fusarium* fungal cell filtrate to different temperatures. Time was held constant for an hour while the concentration of silver nitrate was maintained at 2 mM. The contact ratio of one is to one between the silver nitrate solution and the *Fusarium* fungal cell filtrate was as well maintained. Temperatures 60 °C, 70 °C and 80 °C were investigated and at the end of each investigation the absorbance and spectrums associated with each reaction were recorded [28].

Synthesis of nanoparticles using the fungal cell filtrate time was varied at different intervals for a period of five hours. A ratio of one is to one between the silver nitrate solution and the *Fusarium* cell filtrate was used in the investigation at a contact temperature of 80 °C. The concentration of the silver nitrate solution was held constant at 2 mM. After thirty minutes, one hour, two hours, three hours, four hours and five hours aliquots were taken and each time the absorbance and the spectrums obtained were recorded [29].

## 2.5 Characterization of the silver nanoparticles

The spectral data were acquired using an IRAffinity-1S FTIR spectrophotometer (Shimadzu Corp., 03191) equipped with an ATR. The instrument was set up to perform a total of 20 scans with 4 cm<sup>-1</sup> spectral resolution for both background and sample spectra, recorded rapidly at the range between 4000 and 400 cm<sup>-1</sup> [30]. The X-ray diffractograms were obtained using a Bruker D8 Advance Diffractometer (Bruker, Ettlingen, Germany) with a copper tube operating at a voltage and current of 40 kV and 40 mA. The samples were irradiated with a monochromatic CuK $\alpha$  radiation of 0.1542 nm and the diffractograms were acquired between 2 $\theta$  values of 5°–90° at 0.05° intervals with a measurement time of 1 s per 2 $\theta$  intervals

**Fig. 1** Appearance on compound Microscope X40



**Fig. 2** Appearance on PDA



[31]. The elemental mapping of the nanoparticles were obtained with a Thermo Fischer SEM FEIXL30SFEG equipped with an Oxford Aztec advanced system equipped with an X-MAX 150 mm<sup>2</sup> Silicon Drift Detector [32, 33].

## 2.6 Disc diffusion assay

The synthesised silver nanoparticles were screened for their antimicrobial activity against *Pseudomonas aeruginosa* (ATCC-27853), *Escherichia coli* (ATCC-25922), *Staphylococcus aureus*, (ATCC-25923), and *Bacillus subtilis* (ATCC 23857) using disc diffusion method in Medical Microbiology Department, J.K.U.A.T [34]. Inoculum suspension (108 CFU/ML) were spread over the nutrient agar surface by sterile collection swab and 6 mm *Fusarium sp.* AgNPs, discs sterilized at 120 °C for 15 min were placed onto the petri dishes using flamed forceps and incubated at 37 °C for 24 h [34].

## 3 Results and discussion

### 3.1 Characterization and fungal biomass production

The results from *Fusarium sp.* characterization were obtained and are as depicted below. The initial figure (Fig. 1) shows the appearance of the *Fusarium sp.* on the microscope at a magnification of X40 while the second (Fig. 2) shows its appearance on the potato dextrose agar (Fig. 3).

After the elapse of the 10 days growth of the fungal strain on the Potato Dextrose Agar *Fusarium sp.* was characterised and identified by a deep rose-coloured centre with a pink periphery appearance on the PDA plates. The microscopic studies showed several-celled macroconidia, slightly curved at the pointed ends, a typical canoe-shaped characteristic of a *Fusarium sp.* [35, 36]. The fungal biomass production from the *Fusarium sp.* yielded 43 g wet weight of biomass which was a floating mass on the potato dextrose broth.

### 3.2 Synthesis of *Fusarium sp.* silver nanoparticles

The following images depict the colour changes during the synthesis process.

**Fig. 3** Cell filtrate solution

The image taken at the end of synthesis showed a notable brown solution (Fig. 5), the brown solution was a representation of the colour associated with the synthesised silver nanoparticles [37]. The silver nitrate solution when combined with the *Fusarium sp.* fungal cell filtrate emerged as a colourless solution (Fig. 4) just as the *Fusarium sp.* cell filtrate (Fig. 3) was on its own [38]. Gomathi et al., Lokhande et al., and Abd El-Aziz et al., in their studies with silver nanoparticles obtained a brown colour solution of silver nanoparticles that corresponded to the one obtained in this study [39–41]. This gave confidence in the results since the notable brown colour confirmed the presence of silver nanoparticles.

### 3.2.1 Metal solution and cell filtrate variation.

Following figure shows the results of the combination of the silver nitrate solution and the *Fusarium* fungal cell filtrate (Fig. 5).

From the ratios investigated in this study (Fig. 6) a one is to one ratio between the silver nitrate solution and the *Fusarium sp.* fungal cell filtrate proved to be the best, with the highest peak and a wavelength of 423 nm [42]. The wavelength was characteristic to that of silver nanoparticles. A one is three ratio had the lowest peak an indication of the least concentration of silver nanoparticles among the ratios investigated. The optimum ratio from the study under investigation with *Fusarium sp.* was a one is to one ration which was subsequently employed in the subsequent investigations. It was concluded that a good balance between the cell filtrate and the metal solution was achieved at the ratio of one is to one [25].

**Fig. 4** Metal solution and cell filtrate



### 3.2.2 Variation of metal solution concentration

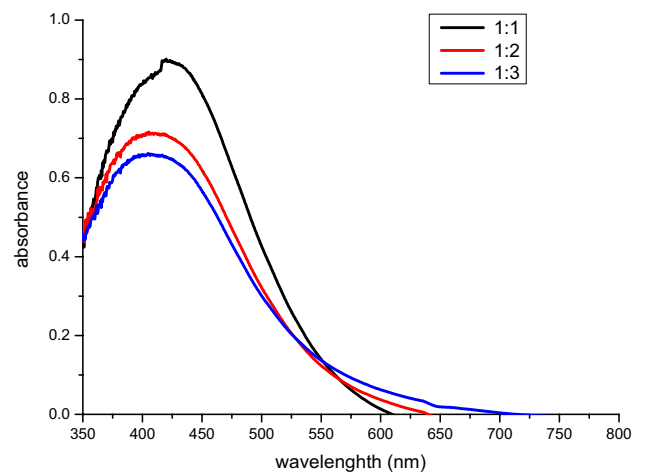
The following is a visual presentation of results obtained after reacting the *Fusarium sp.* fungal cell filtrate with different concentrations of the silver nitrate solution.

Of the three concentrations investigated (Fig. 7) 2 mM concentration showed the highest peak at an absorbance of 0.7 and a silver nanoparticles characteristic wavelength of 418 nm [43]. The 1 mM concentration was the furthest from the optimum concentration as it gave the lowest peak. The wavelength of 418 nm at the optimum concentration confirmed the presence of silver nanoparticles as the wavelength lied within the SPR associated with the nanoparticles [44]. The highest peak obtained at 2 mM showed that more of the nanoparticles got produced at this concentration as compared to when 1 mM or 1.5 mM concentrations were being employed (Fig. 7). This as well confirmed that beer lamberts law was being obeyed by the synthesis reactions [45].

### 3.2.3 Variation of temperature

The following figure is a representation of results obtained by reacting the optimum combination ratio of the silver nitrate solution with *Fusarium sp.* fungal cell filtrate at different temperatures.

Of the temperatures 60 °C, 70 °C and 80 °C investigated, 80 °C stood out as the most suitable temperature in synthesising the silver nanoparticles using the *Fusarium sp.* fungal cell filtrate. It had the highest peak with a wavelength of 432 nm (Fig. 8) [46] which fell well within the SPR of silver nanoparticles, this confirmed the presence of synthesised silver nanoparticles [46]. It was noted that as temperature increased the nanoparticles were being produced at a quick speed. Temperature was believed to increase the number of collision between the cell filtrate and the silver nitrate solution. Increased number of collisions increased the interactions between the filtrate and the metal solution making the reduction of silver ions to silver nanoparticles faster [47].

**Fig. 5** Nanoparticles solution**Fig. 6** UV-Vis spectra of AgNPs obtained from varying the combination ratios

### 3.2.4 Variation of time

The following figure is a graphical depiction of the results obtained by varying reaction time of the *Fusarium* fungal cell filtrate and the silver nitrate metal solution.

After 30 min of contacting the *Fusarium sp.* cell filtrate with the silver nitrate solution a small broad peak emerged at around 446 nm [48] (Fig. 9) an indication of synthesis in the early stages. As reaction time was increased the peaks

**Fig. 7** UV-Vis spectra of AgNPs obtained from varying the contact concentration

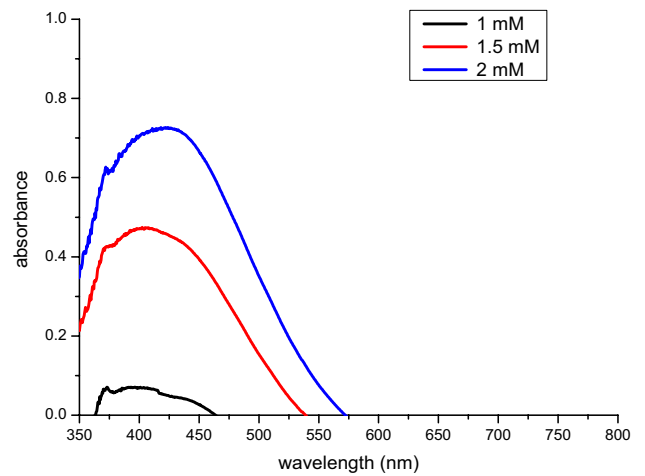


**Fig. 8** UV-Vis spectra of AgNPs obtained from varying the contact temperature

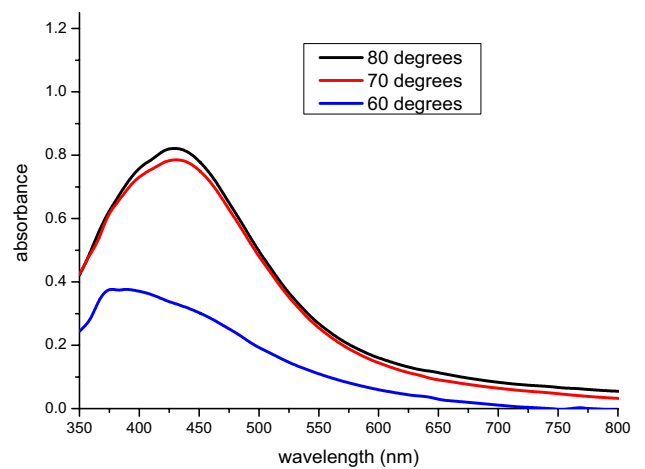
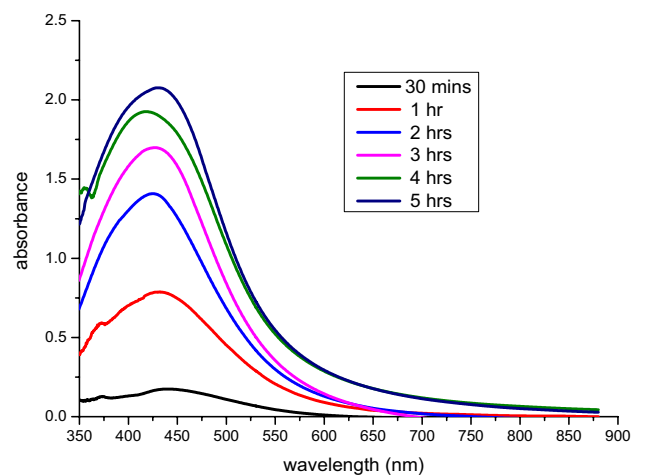


**Fig. 9** UV-Vis spectra of AgNPs obtained from varying the contact time



grew narrow compared to initial peaks that were broad. The highest peak emerged after five hours at a wavelength of 434 nm which was characteristic to silver nanoparticles SPR. This confirmed that the produced nanoparticles were indeed



**Fig. 10** FTIR spectra of *Fusarium sp* silver nanoparticles

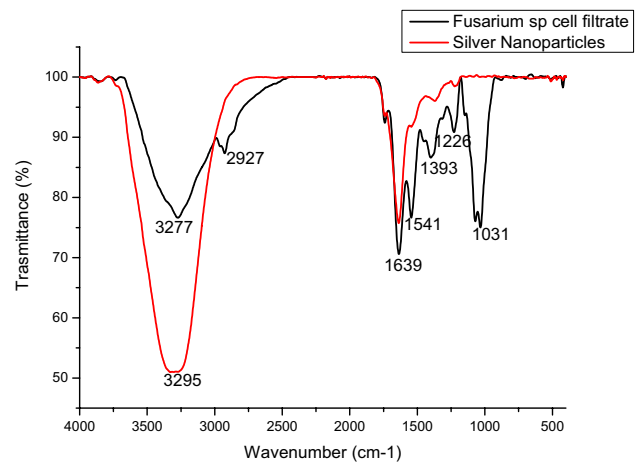
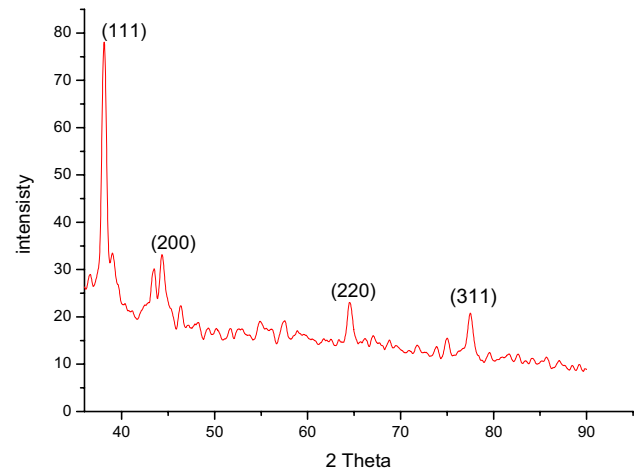


**Fig. 11** X-ray diffractograms of *Fusarium sp.* AgNPs



silver nanoparticles [49]. It was believed as the peak grew narrow from the initial broad peak the concentration of the synthesised silver nanoparticles increased [50].

### 3.3 FTIR analysis of *Fusarium sp.* nanoparticles

The figure below is a visual depiction of the results obtained from FTIR for the investigation involving *Fusarium sp.* fungal strain.

In order to determine the functional groups present in the *Fusarium* cell filtrate and those that remained in the silver nanoparticles after synthesis FTIR analysis (Fig. 10) was carried out for both the cell filtrate and the silver nanoparticles [51]. The wave numbers  $3277\text{ cm}^{-1}$  and  $3295\text{ cm}^{-1}$  were associated with  $\text{-OH}$  stretching [38]. Wave number  $2927\text{ cm}^{-1}$  was attributed to  $\text{C-H}$  stretching of methyl groups found in proteins [52]. The stretches at  $1541\text{ cm}^{-1}$  and  $1639\text{ cm}^{-1}$  represented amide I ( $\text{-C=O}$ ) and amide II ( $\text{-NH}_2$ ) bands respectively [53, 54]. The stretching at wave number  $1393\text{ cm}^{-1}$  was due to a  $\text{C=O}$  stretching of carboxylic group [55]. Wave numbers  $1226\text{ cm}^{-1}$  and  $1031\text{ cm}^{-1}$  revealed the presence of carbohydrate and  $\text{C-OH}$  vibrations of proteins [55, 56].

### 3.4 X-ray diffraction analysis of *Fusarium sp.* AgNPs

The figure below is a visual depiction of the diffractograms obtained from XRD analysis.

The XRD pattern of the *Fusarium sp.* silver nanoparticles suggested that the structure of the nanoparticles is a face centred cubic structure. The diffractogram peaks at  $38^\circ$ ,  $44^\circ$ ,  $64^\circ$ , and  $77^\circ$  were found to correspond to (111), (200), (220) and (311) crystallographic planes attributed to a face centred cubic structure as per JCPDS index [57–59]. In their work Nyabola et al., established that peaks  $38^\circ$  and  $44^\circ$  were a true indication of the presence of silver nanoparticles. From

**Fig. 12** Nanoparticles appearance on Scanning Electron Microscope

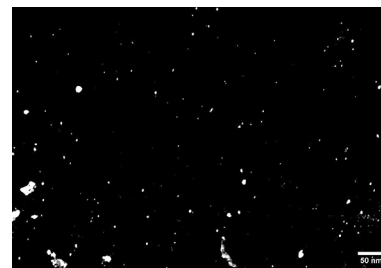
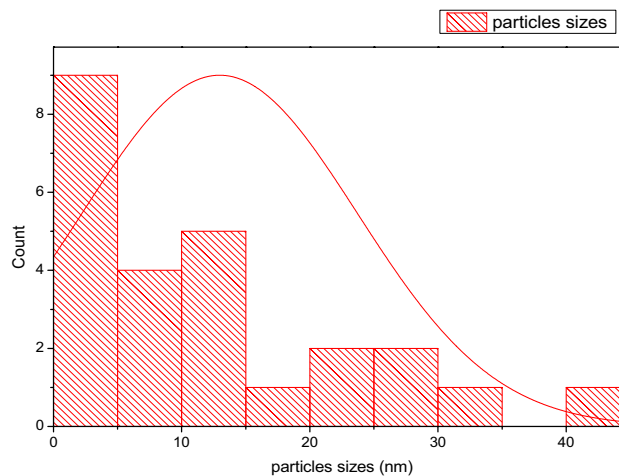


**Fig. 13** Histogram showing the nanoparticle size distribution



the X-ray diffractogram of silver nanoparticles (Fig. 11) it was concluded that the synthesised silver nanoparticles were indeed crystalline in their nature [31]. In their works with silver nanoparticles Rudrappa et al., and Sathiyamoorthi et al., obtained nearly identical results with the ones reported in this study [58, 59]. The crystallite size from the X-ray diffraction data was found to be 38.5 nm, the crystalline size of the nanoparticles was determined by the use of Debye Scherrer's equation as follows:

$$D = \left( \frac{K\lambda}{\beta \cos\theta} \right) \quad (1)$$

where  $D$  is the average particle size (nm),  $K$  is a constant equal to 0.94,  $\lambda$  is the wavelength of X-ray radiation,  $\beta$  is full-width at half maximum of the peak in radians, and theta is the diffraction angle (degree) (Eq. (1)) [60, 61]. In their studies with silver nanoparticles Absi et al., found silver nanoparticles with a crystallite size similar to that obtained in the current study [62]. In another study carried out by Singh et al., they obtained silver nanoparticles with a crystallite size identical to the value obtained from the current investigation [63].

### 3.5 Scanning electron microscope analysis of *Fusarium* sp. AgNPs

The results from the scanning electron microscope (Fig. 12) indicated that the synthesised silver nanoparticles were spherical in nature and had an average size of 12 nm (Fig. 13). In their study using a *Fusarium* species Gudikandula et al., obtained silver nanoparticles that were spherical in nature with an average size of 16 nm [64]. The smaller the nanoparticle sizes are, the more efficient they become when it comes to their application as antimicrobial agents [65]. In a study by Singh et al., silver nanoparticles ranging between 12 to 20 nm with an average size of 16 nm were synthesised with the help of an endophytic fungus *Fusarium semitectum* [66]. The results from these studies related well with the current study.

### 3.6 Stability of the *Fusarium* sp. silver nanoparticles

The following figures visually present the stability results of the silver nanoparticles over a period of three months.

**Fig. 14** Stability of the silver nanoparticles on day one

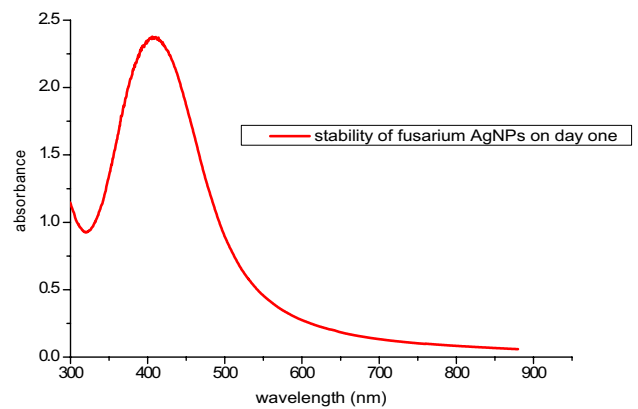


**Fig. 15** Stability of the silver nanoparticles after one month

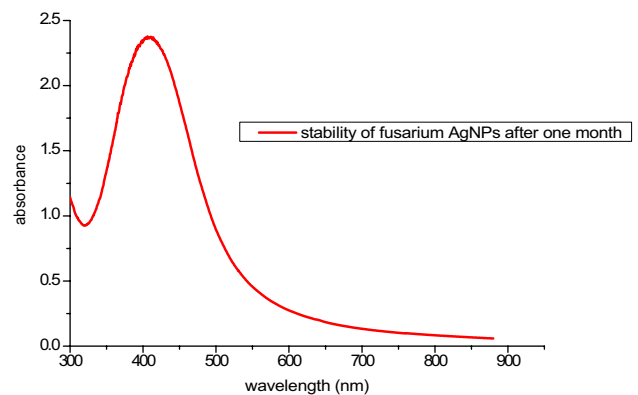
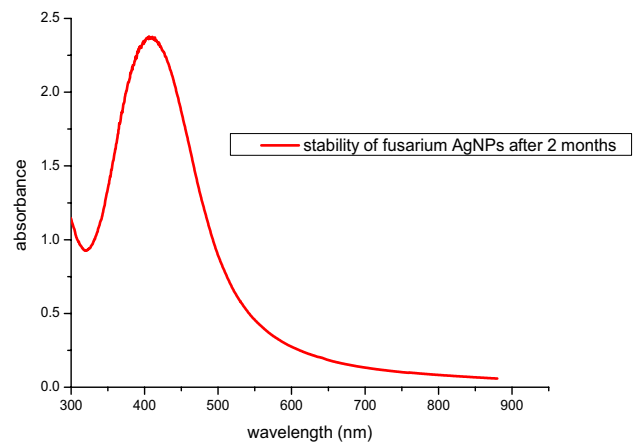


**Fig. 16** Stability of the silver nanoparticles after two months



The stability spectrums (Figs. 14, 15, 16 and 17) indicated that the nanoparticles remained stable over the whole monitoring period. The UV–VIS spectrums showed the same sharp curve as it was taken on day one [67]. This was an indication that after three months the silver nanoparticles were still stable and neither had they reduced in concentration nor agglomerated. Had there been an agglomeration it would be expected that a red shift commonly known as a bathochromic shift could have emerged. This could have been a shift towards higher wavelengths. Had there been a decrease in the concentration of the silver nanoparticles a hypochromic shift would have been expected. This could have been a shift towards lower absorbance values [68]. The fact that the nanoparticles showed stability indicated that their application is effective and long lasting.

**Fig. 17** Stability of the silver nanoparticles after three months

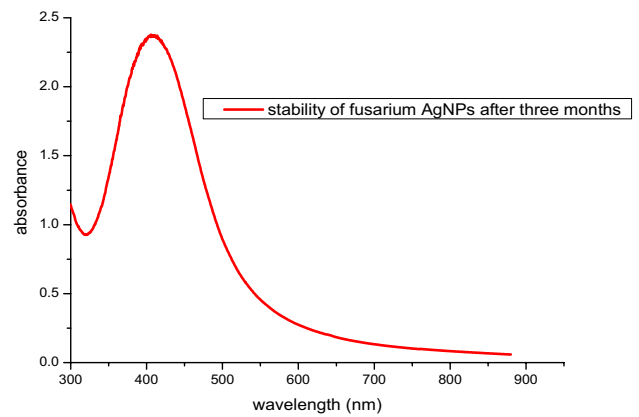
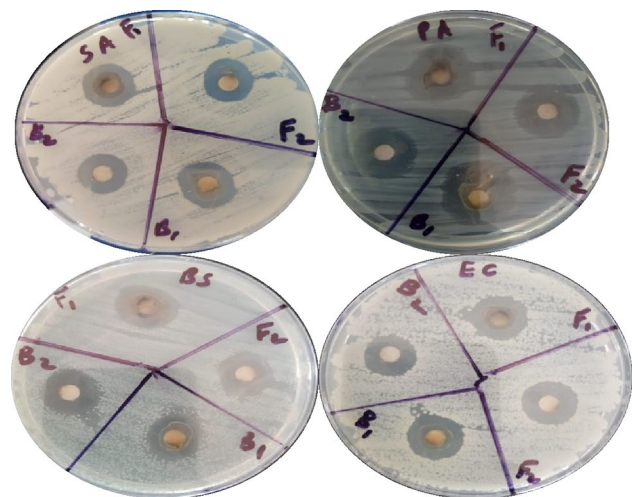


**Table 1** Depicting antimicrobial results

Microorganism	<i>S. aureus</i>	<i>E. coli</i>	<i>P. aeruginosa</i>	<i>B. subtilis</i>
1 mM	No inhibition	No inhibition	No inhibition	No inhibition
10 mM	11 ± 0.6 mm	10 ± 0 mm	9 ± 0.6 mm	12 ± 0.6 mm
20 mM	17 ± 0 mm	15 ± 0.6 mm	16 ± 0.6 mm	17 ± 0.6 mm
100 mM	17 ± 0.6 mm	16 ± 0.6 mm	16 ± 0 mm	17 ± 0.6 mm

**Fig. 18** Antimicrobial assay images



### 3.7 Antimicrobial analysis

Antimicrobial studies showed promising results of the *Fusarium sp.* silver nanoparticles against the four disease causing microorganisms that were under investigation. As illustrated by the table below (Table 1) at 1 mM concentration there was no inhibition but on increasing the concentration to 10 mM inhibition was notable. At 20 mM and 100 mM the inhibition exhibited by the two concentrations increased but was almost similar (Table 1) (Fig. 18). In their works with silver nanoparticles Nyabola et al., synthesised silver nanoparticles using a green method and after investigating the antimicrobial potency, inhibition zones of 10–19 mm against *Staphylococcus aureus*, *Escherichia coli*, *Pseudomonas aeruginosa* and *Bacillus subtilis* were realised [31]. In an investigation conducted by Gholami-Shabani et al., silver nanoparticles were produced using the fungus *Fusarium oxysporium*, the inhibition zones from the study ranged between 14 to 25 mm against *Staphylococcus aureus*, *Escherichia coli* and *Pseudomonas aeruginosa* [69]. Procedures carried out on the antibacterial properties of silver nanoparticles by Muhammad et al., revealed that silver nanoparticles had inhibition zones ranging from 12 to 18 mm against *Escherichia coli* and *Staphylococcus aureus* [70]. The results obtained from these studies resonated well with results obtained from the current study.

## 4 Conclusion

From the investigations conducted it is clear that silver nanoparticles synthesised from *Fusarium sp.* possess good and promising antimicrobial potency. The investigations also revealed that the synthesised silver nanoparticles remained stable after synthesis. The ability of the silver nanoparticles to retain stability and still maintain its antimicrobial properties indicated that the silver nanoparticles can be applied as antimicrobials. Going forward into the future when well configured the silver nanoparticles obtained from the green method using *Fusarium sp.* can be applied as active agents in antimicrobial surface coatings, there by assist in reducing infections and use of antibiotics hence countering the threat of antimicrobial resistance.

**Acknowledgements** The authors take this opportunity to acknowledge the financial support of Africa-ai-Japan for the financial year 2023/24. They also acknowledge the support of chemistry department, Jomo Kenyatta University of Agriculture and technology where much of this work has been carried out.

**Author contributions** NVM Visualised, conceptualized, interpreted, organised and drafted the manuscript. SEM Assisted in Visualisation. MK Assisted in conceptualization. MCW Assisted and advised on antimicrobial studies. ISW Assisted and advised on characterisation. MDN Advised on interpretation and organisation of the manuscript. WW Supervision.

**Funding** The consumables in this study were funded by Africa-ai-japan in their 2023/24 financial year.

**Availability of data and materials** The datasets used and/or analyzed during the current study available from the corresponding author on reasonable request.

## Declarations

**Competing interests** The authors declare that they have no competing interests.

**Open Access** This article is licensed under a Creative Commons Attribution 4.0 International License, which permits use, sharing, adaptation, distribution and reproduction in any medium or format, as long as you give appropriate credit to the original author(s) and the source, provide a link to the Creative Commons licence, and indicate if changes were made. The images or other third party material in this article are included in the article's Creative Commons licence, unless indicated otherwise in a credit line to the material. If material is not included in the article's Creative Commons licence and your intended use is not permitted by statutory regulation or exceeds the permitted use, you will need to obtain permission directly from the copyright holder. To view a copy of this licence, visit <http://creativecommons.org/licenses/by/4.0/>.

## References

1. Dadgostar P. Antimicrobial resistance: implications and costs. *Infect Drug Resist.* 2019;12:3903–10. <https://doi.org/10.2147/IDR.S234610>.
2. Huemer M, Mairpady Shambat S, Brugger SD, Zinkernagel AS. Antibiotic resistance and persistence—implications for human health and treatment perspectives. *EMBO Rep.* 2020;21(12):1–24. <https://doi.org/10.15252/embr.202051034>.
3. Ahmad M, Khan AU. Global economic impact of antibiotic resistance: a review. *J Glob Antimicrob Resist.* 2019;19:313–6. <https://doi.org/10.1016/j.jgar.2019.05.024>.
4. Aguilar GR, et al. The burden of antimicrobial resistance in the Americas in 2019: a cross-country systematic analysis. *Lancet Reg Heal - Am.* 2023. <https://doi.org/10.1016/j.lana.2023.100561>.
5. Akbar S, et al. An overview of the plant-mediated synthesis of zinc oxide nanoparticles and their antimicrobial potential. *Inorg Nano-Metal Chem.* 2020;50(4):257–71. <https://doi.org/10.1080/24701556.2019.1711121>.
6. Crisan MC, Teodora M, Lucian M. Copper nanoparticles: synthesis and characterization, physiology toxicity and antimicrobial applications. *Appl Sci.* 2022;12(141):1–18.
7. Kambale EK, et al. Green synthesis of antimicrobial silver nanoparticles using aqueous leaf extracts from three Congolese plant species (*Brillantaisia patula*, *Crossopteryx febrifuga* and *Senna siamea*). *Heliyon.* 2020;6:e04493. <https://doi.org/10.1016/j.heliyon.2020.e04493>.
8. Hérault N, et al. Silver-containing titanium dioxide nanocapsules for combating multidrug-resistant bacteria. *Int J Nanomed.* 2020;15(15):1267–81. <https://doi.org/10.2147/IJN.S231949>.
9. Madivoli ES, Schwarte JV, Kareru PG, Gachanja AN, Fromm KM. Stimuli-responsive and antibacterial cellulose-chitosan hydrogels containing polydiacetylene nanosheets. *Polymers (Basel).* 2023;15(5):1062. <https://doi.org/10.3390/polym15051062>.
10. Madivoli E. Polysaccharide based hydrogels in drug delivery systems, wound healing, and agriculture. *Chem Africa.* 2023. <https://doi.org/10.1007/s42250-023-00689-1>.
11. Ahmad N, et al. Antimicrobial efficacy of *Mentha piperata*-derived biogenic zinc oxide nanoparticles against UTI-resistant pathogens. *Sci Rep.* 2023;13(1):1–16. <https://doi.org/10.1038/s41598-023-41502-w>.
12. Slavin YN, Asnis J, Häfeli UO, Bach H. Metal nanoparticles : understanding the mechanisms behind antibacterial activity. *J Nanobiotechnology.* 2017;15(65):1–20. <https://doi.org/10.1186/s12951-017-0308-z>.
13. Saqib S, et al. Bimetallic assembled silver nanoparticles impregnated in aspergillus fumigatus extract damage the bacterial membrane surface and release cellular contents. *Coatings.* 2022;12(10):1–15. <https://doi.org/10.3390/coatings12101505>.

14. Mazur P, Skiba-Kurek I, Mrowiec P, Karczewska E, Drożdż R. Synergistic ros-associated antimicrobial activity of silver nanoparticles and gentamicin against staphylococcus epidermidis. *Int J Nanomed*. 2020;15:3551–62. <https://doi.org/10.2147/IJN.S246484>.
15. Hamida RS, Ali MA, Goda DA, Khalil MI, Al-Zaban MI. Novel Biogenic silver nanoparticle-induced reactive oxygen species inhibit the biofilm formation and virulence activities of methicillin-resistant staphylococcus aureus (MRSA) Strain. *Front Bioeng Biotechnol*. 2020;8:1–14. <https://doi.org/10.3389/fbioe.2020.00433>.
16. Ibrahim S, El-Naggar ME, Youssef AM, Abdel-Aziz MS. Functionalization of polystyrene nanocomposite with excellent antimicrobial efficiency for food packaging application. *J Clust Sci*. 2020;31(6):1371–82. <https://doi.org/10.1007/s10876-019-01748-9>.
17. Baygar T, Sarac N, Ugur A, Karaca IR. Antimicrobial characteristics and biocompatibility of the surgical sutures coated with biosynthesized silver nanoparticles. *Bioorg Chem*. 2019. <https://doi.org/10.1016/j.bioorg.2018.12.034>.
18. Srisod S, Motina K, Inprasit T, Pisitsak P. A green and facile approach to durable antimicrobial coating of cotton with silver nanoparticles, whey protein, and natural tannin. *Prog Org Coat*. 2018;120:123–31. <https://doi.org/10.1016/j.porgcoat.2018.03.007>.
19. Jayakumar A, Radoor S, Nair IC, Siengchin S, Parameswaranpillai J, Radhakrishnan EK. Lipopeptide and zinc oxide nanoparticles blended polyvinyl alcohol-based nanocomposite films as antimicrobial coating for biomedical applications. *Process Biochem*. 2021;102:220–8. <https://doi.org/10.1016/j.procbio.2020.12.010>.
20. Valenzuela L, Iglesias-Juez A, Bachiller-Baeza B, Faraldos M, Bahamonde A, Rosal R. Biocide mechanism of highly efficient and stable antimicrobial surfaces based on zinc oxide-reduced graphene oxide photocatalytic coatings. *J Mater Chem B*. 2020;8(36):8294–304. <https://doi.org/10.1039/d0tb01428a>.
21. Turakhia B, Divakara MB, Santosh MS, Shah S. Green synthesis of copper oxide nanoparticles: a promising approach in the development of antibacterial textiles. *J Coatings Technol Res*. 2020;17(2):531–40. <https://doi.org/10.1007/s11998-019-00303-5>.
22. Acikbas G, Calis Acikbas N. Copper oxide- and copper-modified antibacterial ceramic surface. *J Am Ceram Soc*. 2022;105(2):873–87. <https://doi.org/10.1111/jace.181493>.
23. Akther T, Hemalatha S. Mycosilver nanoparticles: synthesis, characterization and its efficacy against plant pathogenic fungi. *Bionanoscience*. 2019;9(2):296–301. <https://doi.org/10.1007/s12668-019-0607-y>.
24. Mahanty S, et al. Green synthesis of iron oxide nanoparticles mediated by filamentous fungi isolated from Sundarban mangrove ecosystem, India. *Bionanoscience*. 2019;9(3):637–51. <https://doi.org/10.1007/s12668-019-00644-w>.
25. Guilger-Casagrande M, de Lima R. Synthesis of silver nanoparticles mediated by fungi: a review. *Front Bioeng Biotechnol*. 2019;7:1–16. <https://doi.org/10.3389/fbioe.2019.00287>.
26. Hassan SA, Hanif E, Khan UH, Tanoli AK. Antifungal activity of silver nanoparticles from *Aspergillus niger*. *Pak J Pharm Sci*. 2019;32(3):1163–6.
27. Huang W, Fang H, Zhang S, Yu H. Optimised green synthesis of copper oxide nanoparticles and their antifungal activity. *Micro Nano Lett*. 2021;16(7):374–80. <https://doi.org/10.1049/mna2.12060>.
28. Naimi-Shamel N, Pourali P, Dolatabadi S. Green synthesis of gold nanoparticles using *Fusarium oxysporum* and antibacterial activity of its tetracycline conjugant. *J Mycol Med*. 2019;29(1):7–13. <https://doi.org/10.1016/j.mycmed.2019.01.005>.
29. Balashanmugam P, Balakumaran MD, Murugan R, Dhanapal K, Kalaichelvan PT. Phytochemical synthesis of silver nanoparticles, optimization and evaluation of in vitro antifungal activity against human and plant pathogens. *Microbiol Res*. 2016;192:52–64. <https://doi.org/10.1016/j.micres.2016.06.004>.
30. Kiprono P, Kiptoo J, Nyawade E, Ngumba E. Iron functionalized silica particles as an ingenious sorbent for removal of fluoride from water. *Sci Rep*. 2023;13(1):1–13. <https://doi.org/10.1038/s41598-023-34357-8>.
31. Nyabola AO, Kareru PG, Madivoli ES, Wanakai SI, Maina EG. Formation of silver nanoparticles via *aspilia plurisetia* extracts their antimicrobial and catalytic activity. *J Inorg Organomet Polym Mater*. 2020;30(9):3493–501. <https://doi.org/10.1007/s10904-020-01497-7>.
32. Kian LK, Jawaid M, Ariffin H, Alotman OY. Isolation and characterization of microcrystalline cellulose from roselle fibers. *Int J Biol Macromol*. 2017;103:931–40. <https://doi.org/10.1016/j.ijbiomac.2017.05.135>.
33. Otenda BV, Kareru PG, Madivoli ES, Salim AM, Gichuki J, Wanakai SI. Starch-hibiscus-cellulose nanofibrils composite films as a model antimicrobial food packaging material. *J Nat Fibers*. 2022. <https://doi.org/10.1080/15440478.2022.2058674>.
34. Madivoli ES, et al. Facile synthesis of silver nanoparticles using *lantana trifolia* aqueous extracts and their antibacterial activity. *J Inorg Organomet Polym Mater*. 2020;30(8):2842–50. <https://doi.org/10.1007/s10904-019-01432-5>.
35. Mugao LG, Birgen JK. Pathogens associated with tomato Post-harvest losses in Mwea, Kenya. *Int J Multidiscip Res Growth Eval*. 2021;2(2):225–32. <https://doi.org/10.54660/ijmrg.2021.2.2.225-232>.
36. Zafar A, Jabeen K, Farooqi J (2017) Practical guide and atlas for the diagnosis of fungal infections. [Online]. Available: <https://ecommons.aku.edu/cgi/viewcontent.cgi?article=1069&context=books>
37. Win TT, Khan S, Fu PC. Fungus- (*Alternaria* sp.) mediated silver nanoparticles synthesis, characterization, and screening of antifungal activity against some phytopathogens. *J Nanotechnol*. 2020;2020:1–9. <https://doi.org/10.1155/2020/8828878>.
38. Rodríguez-Serrano C, et al. Biosynthesis of silver nanoparticles by *Fusarium scirpi* and its potential as antimicrobial agent against uropathogenic *Escherichia coli* biofilms. *PLoS ONE*. 2020;15(3):1–20. <https://doi.org/10.1371/journal.pone.0230275>.
39. Lokhande R, Gedam B, Shah Y, Tandon M, Bansod PY. Rationale for near total thyroidectomy in patients with nodular goitre. *Int J Biomed Adv Res IJBAR Int J Biomed Adv Res J*. 2015;6(605):427–30. <https://doi.org/10.7439/ijbar>.
40. Gomathi M, Prakasam A, Rajkumar PV, Rajeshkumar S, Chandrasekaran R, Anbarasan PM. Green synthesis of silver nanoparticles using *Gymnema sylvestre* leaf extract and evaluation of its antibacterial activity. *South Afr J Chem Eng*. 2020;32(2020):1–4. <https://doi.org/10.1016/j.sajce.2019.11.005>.
41. Abd-El-Aziz ARM, Al-Othman MR, Mahmoud MA, Metwaly HA. Biosynthesis of silver nanoparticles using *Fusarium solani* and its impact on grain borne fungi. *Dig J Nanomater Biostructures*. 2015;10(2):655–62.
42. Mardiyanto M, Apriani EF, Heylken FP. The role of temperature and pH in the synthesis of silver nanoparticles using areca catechu l. seed extract as bioreductor. *Farmacia*. 2023;71(2):244–53. <https://doi.org/10.31925/farmacia.2023.2.3>.
43. Fatima R, Priya M, Indurthi L, Radhakrishnan V, Sudhakaran R. Biosynthesis of silver nanoparticles using red algae *Portieria hornemannii* and its antibacterial activity against fish pathogens. *Microb Pathog*. 2019. <https://doi.org/10.1016/j.micpath.2019.103780>.
44. Meena RK, Meena R, Arya DK, Jadoun S, Hada R, Kumari R. Synthesis of silver nanoparticles by *phyllanthus emblica* plant extract and their antibacterial activity. *Mater Sci Res India*. 2020;17(2):136–45. <https://doi.org/10.13005/msri/170206>.

45. Naseem K, Ur Rehman MZ, Ahmad A, Algarni TS, Dubal D. Plant extract induced biogenic preparation of silver nanoparticles and their potential as catalyst for degradation of toxic dyes. *Coatings*. 2020;10(12):1–15. <https://doi.org/10.3390/coatings10121235>.
46. Yang X, Wu JY. Synthetic conditions, physical properties, and antibacterial activities of silver nanoparticles with exopolysaccharides of a medicinal fungus. *Materials (Basel)*. 2022;15(16):1–10. <https://doi.org/10.3390/ma15165620>.
47. Verma A, Mehata MS. Controllable synthesis of silver nanoparticles using Neem leaves and their antimicrobial activity. *J Radiat Res Appl Sci*. 2016;9(1):109–15. <https://doi.org/10.1016/j.jrras.2015.11.001>.
48. Chandraker SK, Lal M, Kumar A, Shukla R. *Justicia adhatoda* L. mediated green synthesis of silver nanoparticles and assessment of their antioxidant, hydrogen peroxide sensing and optical properties. *Mater Technol*. 2022;37(10):1355–65. <https://doi.org/10.1080/10667857.2021.1949525>.
49. Hamidi A, Taghavizadeh Yazdi ME, Amiri MS, Hosseini HA, Darroudi M. “Biological synthesis of silver nanoparticles in *Tribulus terrestris* L. extract and evaluation of their photocatalyst, antibacterial, and cytotoxicity effects. *Res Chem Intermed*. 2019;45(5):2915–25. <https://doi.org/10.1007/s11164-019-03770-y>.
50. Fahmy HM, et al. Coated silver nanoparticles: synthesis, cytotoxicity, and optical properties. *RSC Adv*. 2019;9(35):20118–36. <https://doi.org/10.1039/c9ra02907a>.
51. Shukla G, Gaurav SS, Singh A, Rani P. Synthesis of mycogenic silver nanoparticles by *Fusarium pallidoroseum* and evaluation of its larvicidal effect against white grubs (*Holotrichia* sp.). *Mater Today Proc*. 2020;49:3517–27. <https://doi.org/10.1016/j.matpr.2021.07.238>.
52. Gupta K, Chundawat TS. Zinc oxide nanoparticles synthesized using *Fusarium oxysporum* to enhance bioethanol production from rice-straw. *Biomass Bioenerg*. 2020;143: 105840. <https://doi.org/10.1016/j.biombioe.2020.105840>.
53. Bunaciu AA, Aboul-Enein HY. Early diseases diagnosis in body fluids (serum and saliva) using infrared spectroscopy. *Appl Chem Eng*. 2023;6(2):2097. <https://doi.org/10.24294/ace.v6i2.2097>.
54. Sogra Fathima B, Balakrishnan RM. Biosynthesis and optimization of silver nanoparticles by endophytic fungus *Fusarium solani*. *Mater Lett*. 2014;132:428–31. <https://doi.org/10.1016/j.matlet.2014.06.143>.
55. Soliman MKY, Abu-Elghait M, Salem SS, Azab MS. Multifunctional properties of silver and gold nanoparticles synthesis by *Fusarium pseudonygamai*. *Biomass Convers Biorefinery*. 2022. <https://doi.org/10.1007/s13399-022-03507-9>.
56. Kim SH, Lahlali R, Karunakaran C, Vujanovic V. Specific mycoparasite-fusarium graminearum molecular signatures in germinating seeds disabled fusarium head blight pathogen's infection. *Int J Mol Sci*. 2021;22(5):1–20. <https://doi.org/10.3390/ijms22052461>.
57. Jabbar AH, et al. Green synthesis and characterization of silver nanoparticle (AgNPs) using pandanus atrocarpus extract. *Int J Adv Sci Technol*. 2020;29(3):4913–22.
58. Rudrappa M, et al. *Plumeria alba*-mediated green synthesis of silver nanoparticles exhibits antimicrobial effect and anti-oncogenic activity against glioblastoma U118 MG cancer cell line. *Nanomaterials*. 2022;12(3):2–19. <https://doi.org/10.3390/nano12030493>.
59. Sathiyamoorthi E, Iskandarani B, Salunke BK, Kim BS. Biomedical potential of silver nanoparticles biosynthesized using gallnut extract. *Green Mater*. 2018;6(2):48–57. <https://doi.org/10.1680/jgrma.17.00032>.
60. Nzilu D, et al. Synthesis and characterization of parthenium hysterophorus - mediated ZnO nanoparticles for methylene blue dye degradation. *J Chem*. 2024;2024:1–19.
61. Nzilu DM, Madivoli ES, Makhani DS, Wanakai SI, Kiprono GK, Kareru PG. Green synthesis of copper oxide nanoparticles and its efficiency in degradation of rifampicin antibiotic. *Sci Rep*. 2023;13(1):1–18. <https://doi.org/10.1038/s41598-023-41119-z>.
62. Absi E, Saleh MA, Al-Hada NM, Hamzah K, Alhawsawi AM, Banoqitah EM. Binary nickel and silver oxides by thermal route: preparation and characterization. *Appl Phys A Mater Sci Process*. 2021;127(8):1–11. <https://doi.org/10.1007/s00339-021-04775-4>.
63. Singh J, et al. Structural investigation and optical properties of silver nanoparticles synthesis by chemical method. *J Nano- Electron Phys*. 2020;12(2):1–4. [https://doi.org/10.21272/JNEP.12\(2\).02006](https://doi.org/10.21272/JNEP.12(2).02006).
64. Gudikandula K, Vadapally P, Singara Charya MA. Biogenic synthesis of silver nanoparticles from white rot fungi: their characterization and antibacterial studies. *OpenNano*. 2017;2:64–78. <https://doi.org/10.1016/j.onano.2017.07.002>.
65. Inam M, et al. Size and shape affects the antimicrobial activity of quaternized nanoparticles. *J Polym Sci Part A Polym Chem*. 2019;57(3):255–9. <https://doi.org/10.1002/pola.29195>.
66. Singh AK, Rathod V, Singh D, Mathew J. Effect of silver nanoparticles (AgNps) produced by an endophytic fungus *Fusarium semitectum* isolated from a medicinal plant *Withania somnifera* (ashwagandha) on seed germination. *Int J Res Stud Agric Sci*. 2016;2(5):6–12. <https://doi.org/10.20431/2454-6224.0205002>.
67. Ahmad M, et al. Biosynthesized silver nanoparticles using *Polygonatum geminiflorum* efficiently control fusarium wilt disease of tomato. *Front Bioeng Biotechnol*. 2022;10:1–13. <https://doi.org/10.3389/fbioe.2022.988607>.
68. Gaikwad SC, et al. Screening of different. *J Braz Chem Soc*. 2013;24(12):1974–82.
69. Gholami-Shabani M, et al. Antimicrobial activity and physical characterization of silver nanoparticles green synthesized using nitrate reductase from *Fusarium oxysporum*. *Appl Biochem Biotechnol*. 2014;172(8):4084–98. <https://doi.org/10.1007/s12010-014-0809-2>.
70. Muhammad Tahir H, et al. Synthesis of sericin-conjugated silver nanoparticles and their potential antimicrobial activity. *J Basic Microbiol*. 2020;60(5):458–67. <https://doi.org/10.1002/jobm.201900567>.